Volume 23, No 2 | International Journal of Radiation Research, April 2025

Dosimetric impact of Acuros XB over Anisotropic analytical algorithm in kilo voltage Cone-beam CT based treatment planning

C.O. Clinto[1,2*] and B. Bindhu[1]

[1]*Department of Physics, Noorul Islam Centre for Higher Education, Kumaracoil, Tamil Nadu, India*
[2]*Department of Radiation Oncology, Aster Medcity, Kochi, Kerala, India*

► ***Original article***

Corresponding author:
C.O. Clinto, M.Sc.
E-mail: *clintoco@gmail.com*

Received: February 2024
Final revised: July 2024
Accepted: August 2024

Int. J. Radiat. Res., April 2025; 23(2): 291-296

DOI: 10.61186/ijrr.23.2.291

Keywords: *Cone-beam computed tomography, Acuros XB, Anisotropic analytical algorithm.*

ABSTRACT

Background: The Cone beam computed tomography (CBCT)-based planning is an effective approach and can act as an indicator for adaptive radiotherapy. This study assesses the dosimetric impact of Acuros in comparison to the anisotropic analytical algorithm (AAA) in kilo voltage-CBCT dose calculation using protocol-specific calibration and Hounsfield unit (HU) override techniques. ***Materials and Methods:*** In this study, three anatomical sites—pelvis, head and neck and thorax—were considered for evaluation. The anthropomorphic phantoms used were the BrainLab pelvis phantom, Accuray's head phantom, and an indigenously developed thorax phantom, respectively. ***Results:*** In the prostate case, the maximum difference between AAA and Acuros was 0.3% for protocol-specific calibration and 0.6% for HU override. In the head and neck case, the differences were 1.1% and 0.9% for the respective techniques. In the study on lung tumors, there was an 8% underestimation in the ipsilateral lung mean dose for the protocol-specific CBCT calibration with Acuros, compared to a 0.6% overestimation with AAA. Compared with the EBT3 film dose profile, the mismatch was evident, with Acuros showing greater accuracy over AAA. ***Conclusion:*** The dosimetric accuracy of CBCT-based dose calculation is affected by the choice of dose calculation algorithm for a given image quality and technique. The effect of the dose calculation algorithm depends on site-specific inhomogeneity: it is least for the pelvic region and significant for the head and neck and thorax regions. Acuros appears to be much more effective than AAA in accounting for the image quality differences of CBCT.

INTRODUCTION

The Cone-beam computed tomography (CBCT) imaging system plays a vital role in image-guided radiotherapy (IGRT). Dose calculation on CBCT images allows for consideration of daily variations in treatment. The concept of feasibility in CBCT-based dose calculation underpins the idea of adaptive radiotherapy [1, 2]. In 2006, Yoo *et al.* [3] investigated the feasibility of dosimetry using CBCT images, sparking significant research interest in the field. Various techniques have evolved, including (1) applying a standard planning computed tomography (CT) calibration curve [4-6], (2) applying a CBCT site-specific calibration curve [5-8], (3) performing a Hounsfield unit (HU) override [9-11], (4) using deformable image registration [6, 12, 13], (5) dose deformation [14-16], and (6) combined techniques [9, 17-19]. In 2020, Giacometti *et al.* [20] reviewed the various approaches and observed that CBCT calculation accuracy depends more on image quality than the method. The large cone geometry of CBCT introduces increased scatter and artifacts, resulting in relatively lower image quality compared to fan-beam CT (FB-CT) [21]. While initial studies were primarily based on standard CBCT images, recent developments have focused on image processing and deep learning-based approaches aimed at enhancing image quality to achieve greater dosimetric accuracy [22-27]. The dosimetric accuracy of CBCT images is influenced by the choice of dose calculation algorithms. A study has compared the performance of different algorithms in CBCT calculations [28]. The selection of the optimal dose calculation algorithm for CBCT-based planning must be validated against different techniques [29].

In the Varian external beam planning system, both the Anisotropic Analytical Algorithm (AAA) and Acuros XB are employed for photon beam calculations [30]. The AAA algorithm is an advanced pencil-beam algorithm that employs multiple pencil-beam dose kernels to model the dose contributions from various radiation sources within a clinical beam. Acuros XB is a photon beam dose calculation algorithm that analytically solves the Linear Boltzmann Transport Equation (LBTE), delivering results comparable to the more time-intensive Monte Carlo calculation models. Several researchers have stated that Acuros

XB provides better accuracy than AAA in the presence of inhomogeneity [30-38]. However, dosimetric accuracy varies with anatomical site and image calibration techniques. In this study, we compared the dose calculation accuracy of Acuros XB with AAA on CBCT images. To the best of our knowledge, this is the first time CBCT-based planning has been validated with different techniques and algorithms.

This study aimed to evaluate the dosimetric impact of Acuros XB (version 13.7.16) compared to AAA (version 13.7.16) in kV-CBCT dose calculation with protocol-specific CBCT calibration and HU override. Both techniques were evaluated for three treatment sites: pelvis, head and neck, and thorax, using anthropomorphic phantoms.

MATERIALS AND METHODS

In this study, anthropomorphic phantoms were used for the evaluation of three anatomical sites: pelvis, head and neck, and thorax. The CT images of 2mm slice thickness acquired using Biograph Horizon PET/CT scanner (Siemens Healthcare Private Limited, India) were taken as standard for all the sites. The CBCT images were acquired using the TrueBeam On-board imaging system (Varian Medical Systems, Palo Alto, CA). The CTP404 module in Catphan® 504 (The Phantom Laboratory, USA) [29] was used for the CT and CBCT calibration of the pelvis and head and neck studies. The Gammex® 467 (GAMMEX, USA) Tissue characterization phantom rods have been used for CT and CBCT calibration of the study on lung tumors.

Site-specific Phantoms

The site-specific phantoms and the dose prescribed to the target are provided in table 1. The prostate case study was performed using the BrainLab pelvis phantom (figure 1A: BrainLab Medical Systems, Westchester, IL, USA). An anthropomorphic head phantom (figure 1B: Accuray Inc., Sunnyvale, CA) was selected for the head and neck case study. A lung tumor case study was performed with an indigenously developed thorax phantom (figure 2). The phantom contains two targets: one with a CC13 (IBA Dosimetry, Germany) 0.13 cc ion chamber and the other with a GAFCHROMIC EBT3 (Ashland Advanced Materials, NJ) film for dosimetry. The material compositions to mimic the anatomy are listed in table 2.

Table 1. Site-specific phantom and target prescription. PTV-planning target volume.

Case	Phantom	Target
Prostate	BrainLab pelvis phantom	PTV 70Gy/28fr
Head and Neck	Accuray head phantom	PTV 66Gy/28fr PTV 60Gy/28fr
Lung tumor	Indigenously developed thorax phantom	PTV 45Gy/3fr

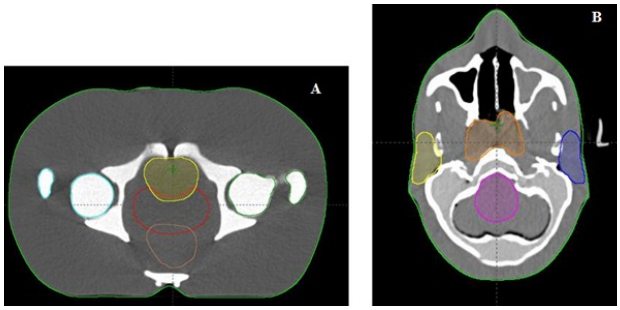

Figure 1. Axial CBCT images of anthropomorphic phantoms with structures used for planning: **(A)** Pelvis Phantom; **(B)** Head Phantom.

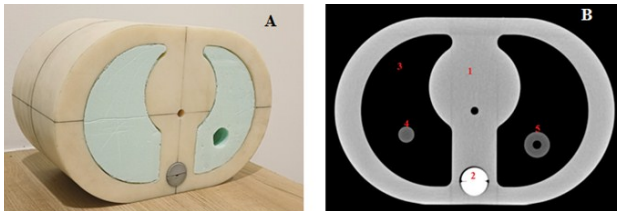

Figure 2. Indigenously developed thorax phantom: **(A)** Physical Image, **(B)** Axial slice of CBCT image.

Table 2. Material composition of indigenously developed thorax phantom (*Refer figure 2B). PA6G- cast polyamide 6, POM- Poly-oxy-methylene, XPS- Extruded Polystyrene.

Organs*	Material	Density g/cm^3
Body (1)	Nylon-6 (PA6G)	1.084
Bone (2)	Delrin (POM)	1.41
Lung (3)	Styrofoam (XPS)	0.05
Target (4 & 5)	Polystyrene	1.05

Protocol-specific CBCT calibration

The calibration curves were created with relative electron density (RED) and physical density (PD) as a function of HU values in the CBCT image. The Catphan 504 was used to generate protocol-specific calibration curves for the pelvis (125 kVp, 1074 mAs, half fan) and head and neck (100 kVp, 270 mAs, full fan). The Gammex 467 tissue characterization phantom rods placed within the thorax phantom were used for the thorax protocol (125 kVp, 270 mAs, half fan).

HU override

In this approach, HU values in the CBCT images were manually assigned based on the mean HU value of corresponding structures in the planning CT. The dose was then calculated on the CBCT images after the HU override with the planning CT calibration curve.

Treatment planning and evaluation

The treatment planning was performed using the Eclipse External Beam Planning system with AAA (version 13.7.16) and Acuros XB (version 13.7.16) (Varian Medical Systems, Palo Alto, CA, USA). The treatment plan on CT images was considered the reference plan for each site. The verification plan was created on CBCT images for the same monitor units (MUs). Both protocol-specific CBCT calibration and

HU override approaches were used for dose calculation on CBCT images. The dose prescribed to the targets for different anatomical sites is provided in table 1. The dose–volume histogram (DVH) parameters of structure sets were compared between the plans on CT and CBCT with both techniques using AAA and Acuros.

The study on lung tumors was performed for two targets: a 3 cm diameter cylindrical target with a CC13 ionization chamber at the center and a 2 cm spherical target with EBT3 film in the mid-plane. The beam arrangement and dose distribution for the 2 cm diameter target in the lung are shown in figure 3. The EBT3 film calibration was done at a 5 cm depth in a slab phantom. The film was scanned using an Epson Expression 10000 XL flatbed scanner. The film calibration and dose profile were obtained using OmniPro-I'mRT (v1.7, IBA Dosimetry, Germany).

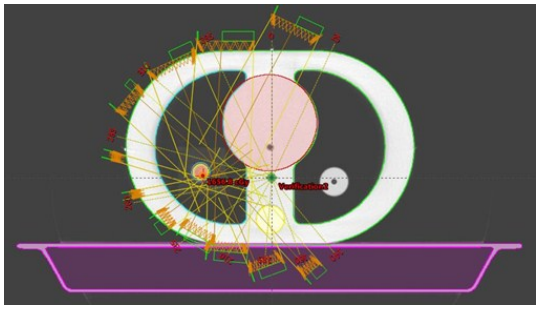

Figure 3. The lung stereotactic body radiation therapy plan of 2cm diameter spherical target.

RESULTS

Study on pelvic tumor

The comparison of DVH parameters of the volumetric modulated arc therapy (VMAT) plans on CT and CBCT is shown in table 3. There was no significant impact observed in using Acuros XB over AAA. There was a noticeable difference observed in estimating mean doses of femoral heads with two different techniques.

Table 3. Comparison of DVH parameters for prostate case. PTV-planning target volume, OARs-organs at risk, D95%-dose received by 95% of volume, Dmax-maximum dose, Dmean-mean dose.

PTV and OARs	Parameters	CT Vs CBCT (Difference in %)			
		Protocol-specific Calibration		HU Override	
		AAA	Acuros XB	AAA	Acuros XB
PTV	D95%	0.60	0.60	0.50	0.5
	Dmax	1.50	1.30	1.30	0.7
Bladder	Dmean	0.70	0.70	0.80	0.9
Rectum	Dmean	2.20	2.50	2.00	2.1
Rt femoral head	Dmean	0.90	1.00	0.20	0.3
Lt femoral head	Dmean	0.40	0.70	-1.00	-0.7

Head and neck study

The comparison of DVH parameters of the VMAT plan on CT and CBCT is shown in table 4. There was a noticeable difference observed with two different algorithms and techniques in estimating the maximum dose to the brainstem.

Table 4. Comparison of DVH parameters for head and neck case. PTV-planning target volume, OARs-organs at risk, D95%-dose received by 95% of volume, Dmean-mean dose, Dmax-maximum dose.

PTV and OARs	Parameters	CT Vs CBCT (Difference in %)			
		Protocol-specific Calibration		HU Override	
		AAA	Acuros XB	AAA	Acuros XB
PTV 66	D95%	-1.50	-1.40	-2.20	-1.8
	Dmax	-0.70	-0.80	-1.20	-1.7
PTV 60	D95%	-2.30	-2.30	-2.50	-2.5
	Dmax	0.30	0.70	-0.10	0.4
Spinal canal	Dmax	3.00	2.90	2.60	2.5
Brainstem	Dmax	0.90	-0.20	0.10	1

Study on lung tumors

In the study on lung tumors, a significant mismatch was observed between the algorithms for both techniques. The comparison of DVH parameters for a 3cm diameter cylindrical target in the thorax phantom is shown in table 5. The protocol-specific calibration technique using AAA has shown a variation of less than 2.8%. While Acuros showed an underestimation of 4% in PTV coverage and 7% in ipsilateral lung mean dose. While comparing with CC13 ionization chamber-measured dose at the centre of the PTV, on the CBCT image, AAA overestimated the dose by 1.4% and Acuros XB by 2.2%.

Table 5. Comparison of DVH parameters for 3cm diameter target in the lung. PTV-planning target volume, OARs-organs at risk, IC-ionization chamber, D95%-dose received by 95% of volume, Dmean-mean dose, Dmax-maximum dose, V20-volume receiving 20Gy.

PTV and OARs	Parameters	CT Vs CBCT (Difference in %)			
		Protocol-specific Calibration		HU Override	
		AAA	Acuros XB	AAA	Acuros XB
PTV	D95%	1.80	-4.00	-2.40	2.5
	Dmax	2.80	1.00	2.00	2.4
CC13 IC	Dmean	1.00	1.10	-0.40	0.7
Ipsilateral Lung-PTV	V20	0.5	-1.8	0.1	1.1
	Dmean	-2.50	-7	1	1.6
Spinal canal	Dmax	1.00	3.80	0.60	3
Heart	Dmean	-1.50	2.00	-1.50	1.5

The comparison of DVH parameters for a 2cm diameter spherical target in the thorax phantom is shown in table 6. The protocol-specific calibration technique using AAA has shown a variation of less than 3%. While Acuros showed a gross underestimation of 8% for the ipsilateral lung mean dose. While comparing with the EBT3 film dose at the center of the target, on the CBCT image, AAA overestimated by 0.7% and Acuros XB underestimated by 0.8%.

The dose profile comparison between AAA and Acuros along the x-axis with protocol-specific calibration is shown in the figure. 4. The Acuros has shown a significant mismatch in the lung-PTV

interface with protocol-specific CBCT calibration. While comparing with EBT3 film-measured dose profile against both CBCT dose calculation techniques (figure 5), a mismatch with protocol-specific CBCT calibration was evident, whereas the HU override technique closely matches the measured dose profile.

Table 6. Comparison of DVH parameters for 2cm diameter target in the lung. PTV-planning target volume, OARs-organs at risk, D95%-dose received by 95% of volume, Dmean-mean dose, Dmax-maximum dose, V20-volume receiving 20Gy.

PTV and OARs	Parameters	CT Vs CBCT (Difference in %)			
		Protocol-specific Calibration		HU Override	
		AAA	Acuros XB	AAA	Acuros XB
PTV	D95%	3.00	1.80	1.40	3
	Dmax	2.80	-2.10	-0.80	0.4
Center	Dmean	0.70	-0.80	-0.40	1
Ipsilateral Lung-PTV	V20	0.8	-0.6	0	0.5
	Dmean	0.60	-8	2.2	1.9
Spinal canal	Dmax	0.30	0.10	-0.30	-1
Heart	Dmean	1.20	-0.60	-0.60	-1.2

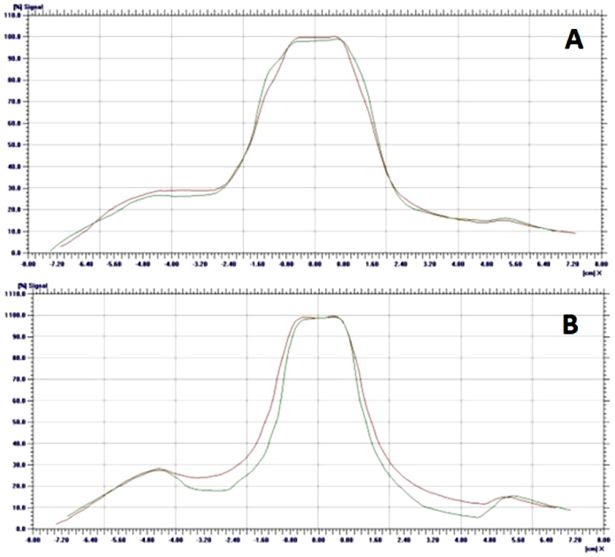

Figure 4. (A) Comparison of dose profiles on CT and CBCT images using AAA. **(B)** Comparison of dose profiles on CT and CBCT images using Acuros XB.

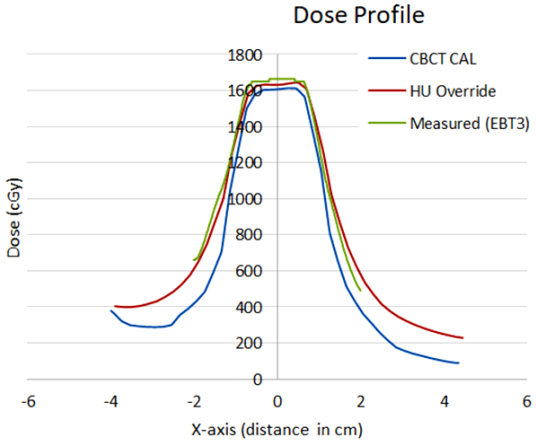

Figure 5. Dose profile comparison on CBCT image using Acuros XB with protocol-specific CBCT calibration and HU override against measurement using EBT3 film.

DISCUSSION

CBCT-based planning is an effective approach and can act as an indicator for adaptive radiotherapy; however, there exist several dosimetric challenges [20]. The dosimetric accuracy of CBCT-based planning is subject to site-specific heterogeneity and image quality [20, 24]. In this study, when using raw CBCT images, the image quality differences from CT were reflected across all sites. Ragab *et al.* [38] also observed higher noise and capping artifacts in CBCT compared to CT images. In the HU override technique, as each structure is assigned the mean HU of the structures in the CT image, it missed out on image detailing, leading to another set of dosimetric inaccuracies.

In the prostate case, the maximum difference between AAA and Acuros was 0.3% for protocol-specific calibration and 0.6% for HU override. In the head and neck case, the differences were 1.1% and 0.9% for the respective techniques. In the study on lung tumors, a significant mismatch was observed between the algorithms for both techniques. For the 2 cm diameter target, there was an 8% underestimation in the ipsilateral lung mean dose for the protocol-specific CBCT calibration technique with Acuros XB compared to a 0.6% overestimation with AAA. However, the impact of Acuros over AAA for the HU override technique was less than 1.6%. There exists a large variation in HU values between the tumor and lung, causing discrepancies in the PTV-lung interface. When compared with the EBT3 film dose profile, a 0.8% underestimation at the center of the target and a mismatch in the lung-PTV interface were evident, as predicted by Acuros over AAA.

Kroon *et al.* [31] observed an underdose of up to 12.3% in lung volumetric modulated arc therapy plans. Kang *et al.* [37] also indicated that Acuros XB was more accurate in the air-phantom interface than AAA by comparing it with film measurement. Abdullah *et al.* [36] also recommended using Acuros XB if the target is involved with tissues of highly different densities. AAA employs a pencil-beam convolution method, which is less advanced in modeling the complex interactions of radiation at interfaces. It simplifies the process by approximating dose distributions using pre-calculated dose kernels. Acuros is founded on the linear boltzmann transport equation, offering a more precise and detailed model of radiation transport. It incorporates advanced heterogeneity correction mechanisms that account for the detailed physical interactions within different tissues, making it more responsive to changes in tissue composition and density. Although AAA accounts for heterogeneity, its approach is more approximate and less detailed compared to Acuros, leading to lower accuracy at interfaces.

Our results confirm the efficacy of Acuros XB in accounting for image quality differences between CT and CBCT. The dosimetric impact was significant in

the presence of highly different tissue densities. Thus, the Acuros XB algorithm should be a better choice for CBCT-based dose planning.

CONCLUSION

The dosimetric accuracy of CBCT-based dose calculation is affected by the choice of dose calculation algorithm for a given image quality and technique. The effect of the dose calculation algorithm depends on the site-specific inhomogeneity: least for the pelvis; significant for the head and neck and thorax region. In the thorax region, AAA fairly predicted the dose to the center of the target, however failed to reflect the dosimetric uncertainty in the lung-PTV interface on the CBCT image with CBCT calibration. The Acuros seems to be much more effective than AAA in accounting for image quality differences of the CBCT.

ACKNOWLEDGEMENTS

We are thankful to Amrita Institute of Medical Sciences, Kochi for providing Accuray's anthropomorphic head phantom. The authors would like to thank Mr. Jaon Bos for his valuable advice.

***Funding*:** This study was supported by no funding.

***Conflicts of interest*:** We wish to confirm that there is no conflict of interest in this study.

***Ethical consideration*:** Phantom study, not applicable.

***Author contribution*:** Study conception and design: C.O.C., B.B.; Data collection: C.O.C.; Manuscript preparation: C.O.C.; Manuscript editing: B.B. Both the authors reviewed the results and approved the final revision of the manuscript.

REFERENCES

1. Sonke JJ, Aznar M, Rasch C (2019) Adaptive radiotherapy for anatomical changes. *Seminars in Radiation Oncology*, ***29****(3): 245-257.*
2. Green OL, Henke LE, Hugo GD (2019) Practical clinical workflows for online and offline adaptive radiation therapy. *Seminars in Radiation Oncology*, ***29****(3): 219-227.*
3. Yoo S and Yin FF (2006) Dosimetric feasibility of cone-beam CT-based treatment planning compared to CT-based treatment planning. *Int J Radiat Oncol, Biol Phys*, ***66****(5): 1553-1561.*
4. Annkah JK, Rosenberg I, Hindocha N, Moinuddin SA, Ricketts K, Adeyemi A, Royle G (2014) Assessment of the dosimetric accuracies of CATPhan 504 and CIRS 062 using kV-CBCT for performing direct calculations. *J Med Phys*, ***39****(3): 133-141.*
5. de Smet M, Schuring D, Nijsten S, Verhaegen F (2016) Accuracy of dose calculations on kV cone beam CT images of lung cancer patients. *Medical Physics*, ***43****(11): 5934.*
6. Giacometti V, King RB, Agnew CE, Irvine DM, Jain S, Hounsell AR, McGarry CK (2019) An evaluation of techniques for dose calculation on cone beam computed tomography. *BJR*, ***92****(1096): 20180383.*
7. Rong Y, Smilowitz J, Tewatia D, Tomé WA, Paliwal B (2010) Dose calculation on kV cone beam CT images: an investigation of the Hu-density conversion stability and dose accuracy using the site-specific calibration. *Medical Dosimetry*, ***35****(3): 195-207.*
8. Jarema T and Aland T (2019) Using the iterative kV CBCT reconstruction on the Varian Halcyon linear accelerator for radiation therapy planning for pelvis patients. *Physica Medica*, ***68***: *112-116.*
9. Onozato Y, Kadoya N, Fujita Y, Arai K, Dobashi S, Takeda K, *et al.* (2014) Evaluation of on-board kV cone beam computed tomography-based dose calculation with deformable image registration using Hounsfield unit modifications. *Int J Radiat Oncol, Biol Phys*, ***89****(2): 416-423.*
10. Rafic KM, Amalan S, Timothy Peace BS, Ravindran BP (2018) Extended localization and adaptive dose calculation using HU corrected cone beam CT: Phantom study. *Reports of Practical Oncology and Radiotherapy,* ***23****(2): 126-135.*
11. Fotina I, Hopfgartner J, Stock M, Steininger T, Lütgendorf-Caucig C, Georg D (2012) Feasibility of CBCT-based dose calculation: comparative analysis of HU adjustment techniques. *Radiotherapy and Oncology*, ***104****(2): 249-256.*
12. Cole AJ, Veiga C, Johnson U, D'Souza D, Lalli NK, McClelland JR (2018) Toward adaptive radiotherapy for lung patients: feasibility study on deforming planning CT to CBCT to assess the impact of anatomical changes on dosimetry. *Physics in Medicine and Biology*, ***63****(15): 155014.*
13. Marchant TE, Joshi KD, Moore CJ (2018) Accuracy of radiotherapy dose calculations based on cone-beam CT: comparison of deformable registration and image correction-based methods. *Physics in Medicine and Biology*, ***63****(6): 065003.*
14. Wen N, Glide-Hurst C, Nurushev T, Xing L, Kim J, Zhong H, *et al.* (2012) Evaluation of the deformation and corresponding dosimetric implications in prostate cancer treatment. *Physics in Medicine and Biology*, ***57****(17): 5361-5379.*
15. Veiga C, Lourenço AM, Mouinuddin S, van Herk M, Modat M, Ourselin S, *et al.* (2015). Toward adaptive radiotherapy for head and neck patients: Uncertainties in dose warping due to the choice of deformable registration algorithm. *Medical Physics*, ***42****(2): 760-769.*
16. Veiga C, Janssens G, Teng CL, Baudier T, Hotoiu L, McClelland JR., *et al.* (2016) First clinical investigation of cone beam computed tomography and deformable registration for adaptive proton therapy for lung cancer. *Int J Radiat Oncol, Biol Phys*, ***95****(1): 549-559.*
17. Moteabbed M, Sharp GC, Wang Y, Trofimov A, Efstathiou JA, Lu HM (2015) Validation of a deformable image registration technique for cone beam CT-based dose verification. *Medical Physics*, ***42****(1): 196-205.*
18. Disher B, Hajdok G, Wang A, Craig J, Gaede S, Battista JJ (2013) Correction for 'artificial' electron disequilibrium due to cone-beam CT density errors: implications for on-line adaptive stereotactic body radiation therapy of lung. *Physics in Medicine and Biology*, ***58*** *(12): 4157-4174.*
19. Schröder L, Stankovic U, Remeijer P, Sonke JJ (2019) Evaluating the impact of cone-beam computed tomography scatter mitigation strategies on radiotherapy dose calculation accuracy. *Physics and Imaging in Radiation Oncology*, ***10***: *35-40.*
20. Giacometti V, Hounsell AR, McGarry CK (2020) A review of dose calculation approaches with cone beam CT in photon and proton therapy. *Physica Medica*, ***76****: 243-276.*
21. Lechuga L and Weidlich GA (2016) Cone beam CT vs. fan beam CT: A comparison of image quality and dose delivered between two differing CT imaging modalities. *Cureus*, ***8****(9): e778.*
22. Meng H, Meng X, Qiu Q, Zhang Y, Ming X, Li Q, *et al*. (2021) Feasibility evaluation of kilovoltage cone-beam computed tomography dose calculation following scatter correction: investigations of phantom and representative tumor sites. *Translational Cancer Research*, ***10****(8): 3726-3738.*
23. Hansen DC, Landry G, Kamp F, Li M, Belka C, Parodi K, Kurz C (2018) ScatterNet: A convolutional neural network for cone-beam CT intensity correction. *Medical Physics*, ***45****(11): 4916-4926.*
24. Rossi M and Cerveri P (2021) Comparison of Supervised and Unsupervised Approaches for the Generation of Synthetic CT from Cone -Beam CT. *Diagnostics (Basel, Switzerland)*, ***11****(8): 1435.*
25. Thing RS, Nilsson R., Andersson S, Berg M, Lund MD (2022) Evaluation of CBCT based dose calculation in the thorax and pelvis using two generic algorithms. *Physica Medica*, ***103****: 157-165.*
26. Joseph J, Singh A, Pournami PN., Jayaraj PB, Puzhakkal N (2023) Cone beam computed tomography enhancement using feature-embedded variational autoencoder with a perceptual loss function. *Int J Imaging Syst Technol,* ***33****(5): 1767-1778*
27. Gong H, Liu B, Zhang G, Dai X, Qu B, Cai B, Xie C, Xu S (2023) Evaluation of dose calculation based on cone-beam CT using different measuring correction methods for head and neck cancer patients. *Technology in Cancer Research Treatment*, ***22****: 15330338221148317.*

28. Title: Evaluations of the dose discrepancies calculated on CT and cone-beam CT using pencil beam convolution and analytical anisotropic algorithms. aapm.org/60-14895-10292-364; Abstract ID: 14895
29. Catphan 504 Manual 2013 (Greenwich, NY: The Phantom Laboratory, Inc.)
30. Tuomas Torsti LK, Petaja V. Using Varian Photon Beam Source Model for Dose Calculation of Small Fields. *Varian Medical Systems; 2013.* (Training material from Varian).
31. Kroon PS, Hol S, Essers M (2013) Dosimetric accuracy and clinical quality of Acuros XB and AAA dose calculation algorithm for stereotactic and conventional lung volumetric modulated arc therapy plans. *Radiation Oncology*, ***8****: 149.*
32. Yan C, Combine AG, Bednarz G, Lalonde RJ, Hu B, Dickens K, *et al*. (2017). Clinical implementation and evaluation of the Acuros dose calculation algorithm. *J Appl Clin Med Phys*, ***18****(5): 195-209.*
33. Seniwal B, Bhatt CP, Fonseca TCF (2020) Comparison of dosimetric accuracy of acuros XB and analytical anisotropic algorithm against Monte Carlo technique. *Biomedical physics engineering express*, ***6*** *(1): 015035.*
34. Gopalakrishnan Z, Bhasi SPR, Menon SVBS, Thayil AG, Nair RK (2022). Dosimetric comparison of analytical anisotropic algorithm and the two dose reporting modes of Acuros XB dose calculation algorithm in volumetric modulated arc therapy of carcinoma lung and carcinoma prostate. *Medical Dosimetry*, ***47****(3): 280-287.*
35. Prasath SS and Ramesh Babu P (2023) Dosimetric comparison between Acuros XB (AXB) and anisotropic analytical algorithm (AAA) in volumetric modulated Arc therapy. *Asian Pacific Journal of Cancer Prevention*, ***24****(5): 1677-1685.*
36. Abdullah C, Farag H, El-Sheshtawy W, Aboelenein H, Guirguis OW (2021) Clinical impact of anisotropic analytical algorithm and Acuros XB dose calculation algorithms for intensity modulated radiation therapy in lung cancer patients. *Journal of X-ray Science and Technology*, ***29****(6): 1019-1031.*
37. Kang SW, Chung JB, Lee JW, Kim MJ, Kim YL, Kim JS, *et al.* (2017) Dosimetric accuracy of the Acuros XB and Anisotropic analytical algorithm near interface of the different density media for the small fields of a 6- MV flattening-filter-free beam. *Int J Radiat Res*, ***15****(2): 157-165.*
38. Ragab H, Abdelaziz DM, Khalil MM, Elbakry MN (2023) Assessment of image quality of two cone-beam computed tomography of the Varian Linear accelerators: Comparison with spiral CT simulator. *Int J Radiat Res,* ***21****(3): 491-497.*